Photoabsorption and Photoionization Studies of Fullerenes and Development of High-Efficiency Organic Solar Cells

Department of Photo-Molecular Science
Division of Photo-Molecular Science III

MITSUKE, Koichiro	Associate Professor
KATAYANAGI, Hideki	Assistant Professor
LE, Hong Quang	Post-Doctoral Fellow
PRAJONGTAT, Pongthep	Research Fellow
MORENOS, Lei Angeli S.	Visiting Scientist
BASHYAL, Deepak	Graduate Student
ASARI, Chie	Technical Fellow
SHIMIZU, Atsuko	Secretary

We have observed the formation of multiply-charged photoions from gaseous fullerenes or aromatic hydrocarbons irradiated with synchrotron radiation at $h\nu$ = 25 to 200 eV. We thus studied the mechanisms and kinetics of consecutive C_2-release reactions on the basis of (i) the yield curves for the fragments $C_{60(70)-2n}^{z+}$ ($n \geq 1$, z = 1–3) as a function of the primary internal energy and (ii) the three dimensional velocity distributions of the fragments. Last year the velocity distributions of C_{60-2n}^{z+} and C_{70-2n}^{z+} were measured for the first time. Concepts of the microcanonical temperature and Arrhenius-type rate constants for individual C_2 ejection steps allowed us to compare the experimental total average kinetic energy with theoretical kinetic energy release predicted from the "model free approach" developed by Klots.

In the second topic we have fabricated dye-sensitized solar cells (DSSCs) containing ruthenium dye and iodide electrolyte and measured their short-circuit current and the intensity of the transmitted light to estimate the wavelength dependence of the incidence photon-to-current conversion efficiency (IPCE) and photoabsorbance (ABS) in the range of 300 to 1000 nm. In addition, we evaluated the quantum yield (APCE) of DSSCs for the electron injection from the excited orbital of Ru dye to the conduction band of TiO_2 nanoparticles. Our final goal is to develop DSSCs with high performance and long lifetime by improving ABS and APCE mainly in the near infrared region.

1. Mass-Analyzed Velocity Map Imaging of Photofragments from C_{70}[1)]

The velocity distributions of the fragments produced by dissociative photoionization of C_{70} have been measured at several photon energies in the extreme UV region, by using a flight-time resolved velocity map imaging (VMI) technique combined with a high-temperature molecular beam and synchrotron radiation. Average kinetic energy release was estimated for the six reaction steps of consecutive C_2 emission, starting from $C_{70}^{2+} \rightarrow C_{68}^{2+} + C_2$ to $C_{60}^{2+} \rightarrow C_{58}^{2+} + C_2$. The total kinetic energy generated in each step shows a general tendency to increase with increasing $h\nu$, except for the first and fifth steps. This propensity reflects statistical redistributions of the excess energy in the transition states for the above fragmentation mechanism. Analysis based on the finite-heat-bath theory predicts the detectable minimum cluster sizes at the end of the C_2–emission decay chain. They accord well with the minimum sizes of the observed ions, if the excess energy in the primary C_{70}^{2+} is assumed to be smaller by ~15 eV than the maximum available energy. The present VMI experiments reveal remarkably small kinetic energy release in the fifth step, in contradiction to theoretical predictions, which suggests involvement of other fragmentation mechanisms in the formation of C_{60}^{2+}.

2. Velocity Map Imaging for Photoionization of Polycyclic Aromatic Hydrocarbons

We have demonstrated the versatility of our apparatus in photoionization study of various nonvolatile substances, by taking an example of complicated dissociation of sumanene $C_{21}H_{12}$ and coronene $C_{24}H_{12}$ in the extreme UV. Though their chemical reactions are sometimes discussed by analogy with those of C_{60}, a great difference in the velocity distribution has been observed between the fragment ions from C_{60} and those from sumanene. The appearance $h\nu$ values for C_{60-2n}^{z+} are higher by 30–33 eV than their thermochemical thresholds for dissociative ionization of C_{60}. Usually, the relative abundance of C_{60-2n}^{z+} is two orders of magnitude lower than that of the parent C_{60}^{z+}. In contrast, the y–t map of sumanene in Figure 1 suggests prompt coulomb explosion of $C_{21}H_{12}^{z+}$ (z = 2 and 3) into singly-charged fragments followed by stepwise C_2 ejection. This argument appears to hold true in the case of photodissociation of coronene $C_{24}H_{12}$.

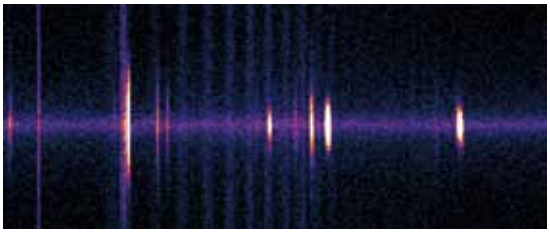

Figure 1. Map of *y*–*t* of the photoions from $C_{21}H_{12}$. The *y* and *t* coordinates are proportional to the *y* component of the ion velocity and the square root of mass-to-charge ratio *m*/*z*, respectively.

3. Photoexcitation and Electron Injection Processes in Azo Dyes Adsorbed on Nanocrystalline TiO_2 Films[3)]

Dye-sensitized solar cells were fabricated using eight azo dyes which have different positions and/or numbers of carboxyl and hydroxyl groups. The short-circuit current density, photoabsorbance, absorptance and quantum yield for dyes-to-TiO_2 electron injection were measured by photons ranging from 380 to 800 nm. X-ray and ultraviolet photoelectron spectroscopy of the photovoltaic electrodes were also conducted. The photon-to-current conversion efficiency of the cells was found to depend mostly on the relative position of the lowest unoccupied molecular orbital of the adsorbed dyes and partly by their concentration on the TiO_2 nanoparticles.

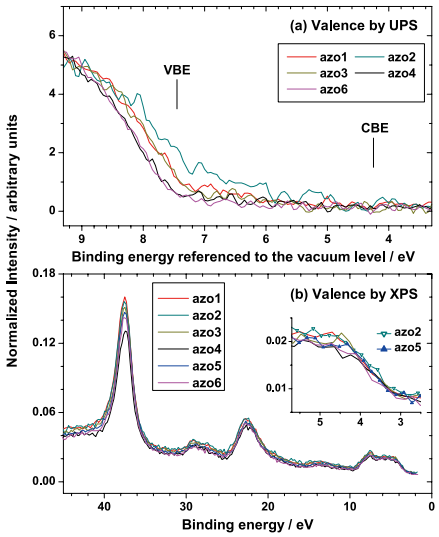

Figure 2. Ionization of valence and Ti 3p electrons of the TiO_2 film covered with six azo dyes on the working electrodes observed by photoelectron spectroscopy.

4. Efficient Dye-Sensitized Solar Cells Made from TiO_2 Nanoparticles Powder, VP P90[4)]

Dye sensitized solar cells (DSSCs) were fabricated by means of a wet process using the paste of titanium dioxide (TiO_2) prepared from commercial powders of TiO_2 nanopartilces, VP TiO_2 P90 and AEROXIDE® TiO_2 P25. The other ingredients of the TiO_2 pastes were ethanol, aqueous solution of acetic acid, α-terpineol, and ethyl cellulose. The optimum composition has been determined by comparing the energy conversion efficiencies of assembled DSSCs. The sensitizer dye is the Ruthenium 535-bisTBA in acetonitrile solution. The conversion efficiency of 9% or higher has been obtained by using a double-layer film of P90-type TiO_2 with an immersion of FTO glass into a $TiCl_4$ solution and an additional coating of a light scattering layer.

5. Fabrication, Analysis and Evaluation of Dye-Sensitized Solar Cells Made from Zinc Oxide Nanorods

Production of zinc oxide nanostructures in solution phase have attracted wide attentions and triggered various research works aiming at low cost and large scale electrode materials for DSSCs. We have studied the growth of ZnO nanorod array on fluorine-doped tin oxide substrates using a low-temperature solution method. By optimizing the growth parameters, such as reagent concentrations and temperatures (typ. 90 °C), we can control the hydrothermal growth and obtain a maximum length of 18 μm with an aspect ratio of 136. The ZnO nanorods were then applied to the electrode materials of the solar cells. The DSSCs with ZnO nanorods have produced the best energy conversion efficiency η of 1.63%. The effects of the difference in aspect ratio and device process on η have been discussed.

6. Theoretical Investigations on the Adsorption Geometries and Electronic Structures of Azo Dyes Adsorbed on TiO_2

We have employed periodic density functional theory calculations to study the adsorption geometries and electronic structures of azo dyes anchored on TiO_2 surfaces. The theoretical adsorption energies indicate that the bidentate bridging configuration is more preferable than the bidentate chelating and monodentate ester-type geometries. The band gap energies are smaller for the adsorbed complexes than for the clean surfaces, since additional electronic states arise from mixing of the molecular orbitals of the dyes with the TiO_2 valence and conduction bands. The strong electronic coupling between the excited states of azo dyes and conduction bands is observed in the high-efficiency dyes, but not in the low-efficiency dyes. Moreover, the Fermi levels of TiO_2 covered with the former dyes are shifted to higher direction than those with the latter. Thus, the open circuit voltage was increased in DSSCs based on the former dyes.

References

1) H. Katayanagi and K. Mitsuke, *J. Chem. Phys.* **135**, 144307 (8 pages) (2011).
2) H. Katayanagi and K. Mitsuke, *J. Chem. Phys. (Communication)* **133**, 081101 (4 pages) (2010).
3) K. Nakajima, K. Ohta, H. Katayanagi and K. Mitsuke, C*hem. Phys. Lett.* **510**, 228–233 (2011).
4) K. Mitsuke, D. Bashyal and K. Nakajima, *Proc. PACCON* **2011**, 457–460 (2011).